© 2016. Published by The Company of Biologists Ltd | Journal of Cell Science (2016) 129, 1477-1489 doi:10.1242/jcs.178608

RESEARCH ARTICLE

The *Drosophila* tricellular junction protein Gliotactin regulates its own mRNA levels through BMP-mediated induction of miR-184

Zohreh Sharifkhodaei[1], Mojgan Padash-Barmchi[1], Mary M. Gilbert[1], Gayathri Samarasekera[1], Tudor A. Fulga[2,*], David Van Vactor[2] and Vanessa J. Auld[1,‡]

ABSTRACT

Epithelial bicellular and tricellular junctions are essential for establishing and maintaining permeability barriers. Tricellular junctions are formed by the convergence of three bicellular junctions at the corners of neighbouring epithelia. Gliotactin, a member of the Neuroligin family, is located at the *Drosophila* tricellular junction, and is crucial for the formation of tricellular and septate junctions, as well as permeability barrier function. Gliotactin protein levels are tightly controlled by phosphorylation at tyrosine residues and endocytosis. Blocking endocytosis or overexpressing Gliotactin results in the spread of Gliotactin from the tricellular junction, resulting in apoptosis, delamination and migration of epithelial cells. We show that Gliotactin levels are also regulated at the mRNA level by micro (mi) RNA-mediated degradation and that miRNAs are targeted to a short region in the 3′UTR that includes a conserved miR-184 target site. miR-184 also targets a suite of septate junction proteins, including NrxIV, coracle and Mcr. miR-184 expression is triggered when Gliotactin is overexpressed, leading to activation of the BMP signalling pathway. Gliotactin specifically interferes with Dad, an inhibitory SMAD, leading to activation of the Tkv type-I receptor and activation of Mad to elevate the biogenesis and expression of miR-184.

KEY WORDS: BMP, miRNA, Tricellular junction

INTRODUCTION

Permeability barriers are essential to prevent fluid flow, and to restrict the diffusion of molecules and pathogens across tissues, such as the epidermis, intestine and brain. Permeability barriers are formed by tight junctions in vertebrates and septate junctions in insects, and the barriers have similar physiological roles and homologous components (Tsukita et al., 2001). Pleated septate junctions form a ladder-like array of electron-dense septa located just below the adherens junction (Tepass and Hartenstein, 1994). Septate junctions comprise an interdependent protein complex, including Neurexin IV (NrxIV) (Baumgartner et al., 1996), Coracle (Fehon et al., 1994), Na^+/K^+ ATPase and Neuroglian (Genova and Fehon, 2003; Paul et al., 2003), Contactin (Faivre-Sarrailh et al., 2004) and Mcr (Batz et al., 2014; Hall et al., 2014). In many epithelia, a specialized junction, the tricellular junction (TCJ), forms at the convergence of the tight junctions or septate junctions from three cells to create a permeability barrier at the corners of neighbouring cells. In *Drosophila*, the TCJ is formed in a range of epithelia and is crucial for septate junction maturation and permeability barrier formation (Fristrom, 1982; Noirot-Timothée et al., 1982; Schulte et al., 2003). Gliotactin (Gli), a single-pass transmembrane protein and a member of the Neuroligin family, is specifically localized to the *Drosophila* TCJ (Schulte et al., 2003). Loss of Gliotactin results in a disruption of the TCJ, the baso-lateral spread of septate junction proteins and a loss of the permeability barrier (Schulte et al., 2003).

Gliotactin protein levels and TCJ localization are tightly controlled by phosphorylation of tyrosine residues and endocytosis (Padash-Barmchi et al., 2010). Overexpressed Gliotactin spreads away from the TCJ and is deleterious, leading to apoptosis, delamination, overproliferation and cell migration in the wing imaginal disc (Padash-Barmchi et al., 2010). Mutation of two conserved tyrosine residues to phenylalanine in Gliotactin disrupts the phosphorylation, endocytosis and subsequent degradation of Gliotactin (Padash-Barmchi et al., 2010). Beyond control at the protein level, Gliotactin has been identified as a potential target of micro (mi)RNAs, with multiple conserved miRNA-target sites predicted in the 3′UTR (Kertesz et al., 2007). Target sequences for one of these microRNAs, miR-184, have been identified in the 3′UTR of other genes coding for septate junction proteins, including NrxIV and Coracle (Kertesz et al., 2007), and have been predicted to exist in a range of other septate junction genes, including the Pasiflora genes (Deligiannaki et al., 2015). However, the role that miR-184 plays in the regulation of Gliotactin and septate junctions *in vivo* has yet to be determined.

Here, we show that Gliotactin mRNA levels are controlled by miR-184-targeted degradation through the 3′UTR. In addition, miR-184 can control the expression level of the core septate junction proteins NrxIV and Coracle, as well as Mcr. We found that overexpressed Gliotactin is the trigger for increased miR-184 expression through activation of the BMP type-1 receptor, Thickveins (Tkv). Moreover, Gliotactin activation of Tkv is through block of the Tkv inhibitor Daughter against dpp (Dad). We conclude that Gliotactin leads to a feedback loop to control Gliotactin mRNA levels thorough Tkv signalling and induction of miR-184.

RESULTS

Overexpression of Gliotactin causes self-downregulation

Gliotactin localization is normally restricted to the TCJ within the columnar epithelia of the wing imaginal disc (Fig. 1A). Overexpression of a full-length Gliotactin transgene causes spread away from the TCJ and around the cell. When driven with *apterous*-GAL4, the pattern of expression is uniform across the dorsal half of the wing imaginal disc (Schulte et al., 2006; Padash-Barmchi et al., 2010). In contrast, when an EP insertion (GliEP) with an upstream activating sequence (UAS) element in the 5′ end of *Gliotactin* was

[1]Department of Zoology, University of British Columbia, Vancouver BC V6T 1Z3, Canada. [2]Department of Cell Biology, Harvard Medical School, Boston, MA 02115, USA.
*Present address: Weatherall Institute of Molecular Medicine, Radcliffe Department of Medicine, University of Oxford, Oxford OX3 9DS, UK.

‡Author for correspondence (auld@zoology.ubc.ca)

Received 11 August 2015; Accepted 11 February 2016

Journal of Cell Science (2016) 129, 1477-1489 doi:10.1242/jcs.178608

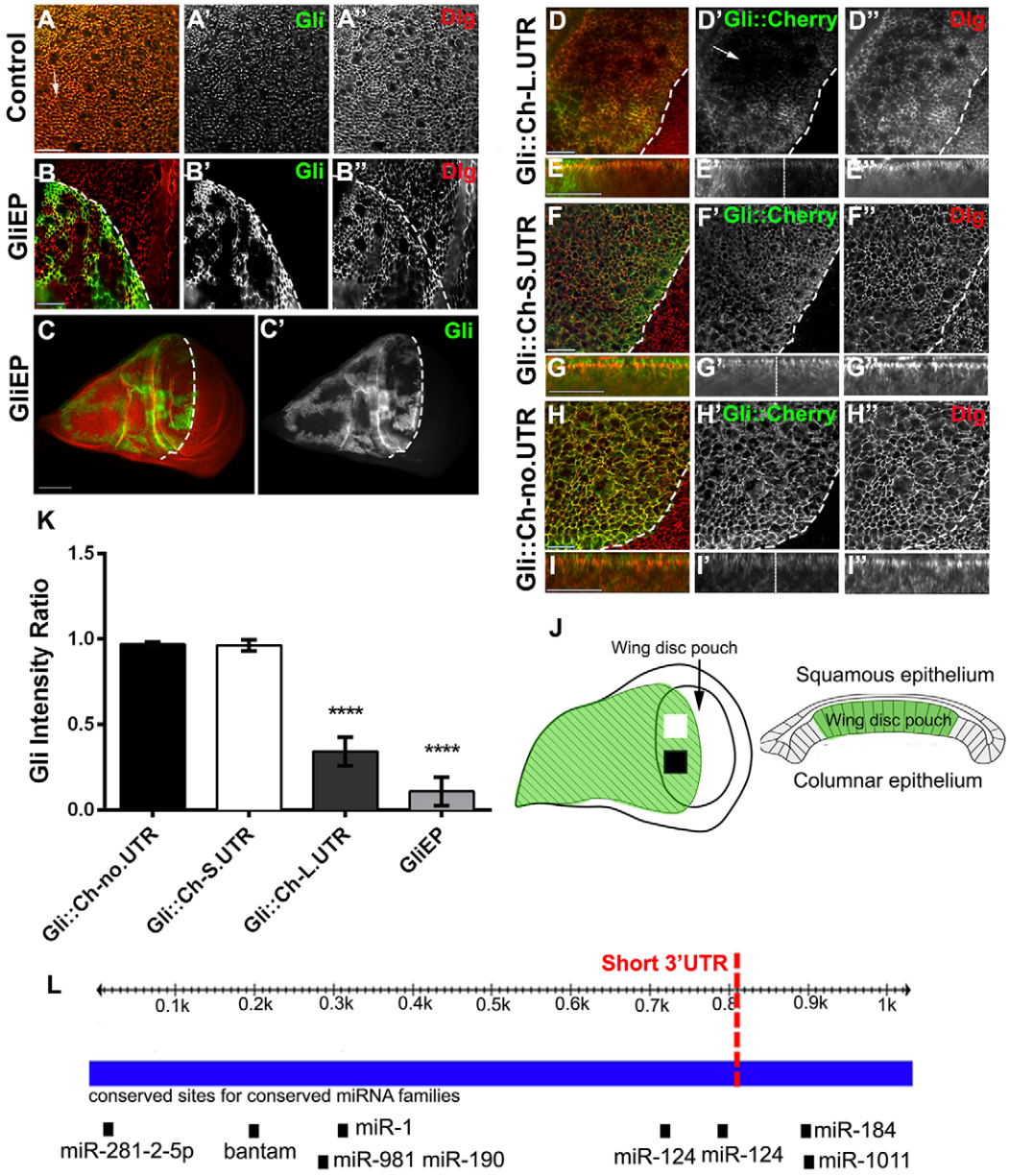

Fig. 1. Overexpression of Gliotactin causes self-downregulation. (A) The expression pattern of Gliotactin in a wild-type wing imaginal disc, immunolabelled for Gliotactin (green, A′) and Dlg (red, A″). Gliotactin was concentrated at the tricellular junction (arrow) and Dlg at the septate junction. (B–H) *apterous*-GAL4-driven expression of Gliotactin transgenes within the wing imaginal disc. The dashed line marks the dorsal–ventral boundary with the dorsal apterous side of the wing imaginal disc to the left. (B,C) High- (B) and low- (C) resolution images of a wing imaginal disc with overexpression of endogenous Gliotactin (green, B′,C′) from an EP (UAS) insertion in *Gliotactin*. Gliotactin was downregulated in a patchy manner, whereas Dlg was not (red, B"). (D) Overexpression of a Gliotactin transgene with the full-length 3′UTR (Gli::Ch-L.UTR) (green, D′) was downregulated (arrow) in regions within the apterous side, whereas Dlg (red, D″) was not. (F–I) Overexpression of Gliotactin with the short 3′UTR (Gli::Ch-S.UTR) or a Gliotactin transgene without a 3′UTR (Gli::Ch-no.UTR). Neither Gliotactin (green, F′,H′) nor Dlg (red, F″,H″) were downregulated. (E,G,I) Side views of the corresponding panels above. (J) Diagram of wing imaginal disc. Fluorescence intensity was measured in two separate areas (squares) in the wing pouch of the apterous side of the imaginal disc (green). A side view of the disc shows the position of the columnar epithelia within the wing pouch. (K) The fluorescence intensity ratio (apterous to wild-type side) of Gli::Ch-L.UTR and GliEP was significantly downregulated in regions across the apterous expression domain compared to the lack of downregulation of Gli::Ch-S.UTR or Gli::Ch-no.UTR (n=10 discs, ****P<0.0001, mean±s.d., one-way ANOVA). (L) The Gliotactin 3′UTR, indicating the conserved miRNA-target sites. Sites for miR-281, bantam, miR-1, miR-981, miR-190, miR-124, miR-1011 and miR-184 are shown, and the dotted line indicates the border of the short and full-length of 3′UTRs observed in Gliotactin-expressed sequence tags. Scale bars: 15 µm (all images except C); 50 µm (C).

driven using *apterous*-GAL4, Gliotactin expression occurred in patches within the dorsal side of the wing disc (Fig. 1B,C). The EP insertion drives the expression of the endogenous Gliotactin mRNA, including the entire 3′UTR, whereas our original UAS-*Gliotactin* transgene lacked the complete 3′UTR, leading to the hypothesis that the differences in expression patterns might reside in the 3′UTR. Using Target Scan Fly (Kheradpour et al., 2007), eight miRNA targets are predicted within the *Gliotactin* 3′UTR that are highly conserved across Drosophilidae species (Fig. 1L). This suggested an additional level of Gliotactin regulation controlled by the 3′UTR. To test this, we expressed a range of transgenes with cherry-tagged *Gliotactin* and different 3′UTR lengths (Fig. S1).

Journal of Cell Science (2016) 129, 1477-1489 doi:10.1242/jcs.178608

These included the entire 3′UTR (Gli::Ch-L.UTR), a short 3′UTR lacking the miR-184- and miR-1011-target sites (Gli::Ch-S.UTR), and finally the SV40 3′UTR lacking all miRNA target sites (Gli::Ch-no.UTR). Transgenic lines overexpressing the entire 3′UTR (Gli::Ch-L.UTR) had regions with reduced levels of Gliotactin protein (Fig. 1D,E) that when measured across different regions in the dorsal side (Fig. 1J) were significantly different (Fig. 1K). This mirrored the patchy pattern observed with the GliEP insertion, although the degree of downregulation was not as strong (Fig. 1K). Transgenes lacking the miR-184- and miR-1011-binding sites (Gli::Ch-S.UTR) (Fig. 1F,G) or the whole 3′UTR (Gli::Ch-no.UTR) (Fig. 1H,I) showed no significant reduction in Gliotactin levels across the *apterous* expression area (Fig. 1K). These results suggest that the 3′UTR and, specifically, miR-184 and/or miR-1011 control Gliotactin levels.

miR-184 controls septate junction proteins and Gliotactin

miR-184 has been identified *in vitro* as a potential regulator of other septate junction proteins, including NrxIV, Coracle and Mcr, in addition to Gliotactin (Kertesz et al., 2007). miR-184 is expressed throughout embryogenesis (Aboobaker et al., 2005; Li et al., 2011) in larval imaginal discs (Li et al., 2011) and plays a role in the regulation of the female germline (Iovino et al., 2009). To test the role of miR-184 in the control of Gliotactin and septate junction proteins, we overexpressed miR-184 in the wing imaginal disc using *apterous*-GAL4. Elevated miR-184 expression caused a downregulation of Gliotactin (Fig. 2A,B) and a reduction of the septate junction proteins NrxIV (Fig. 2C,D), Mcr (Fig. 2E,F) and Coracle (Cora) (Fig. 2G,H). The expression of other junctional proteins, Disc Large (Dlg) (Fig. 2A), E-cadherin (Ecad) and Fasciclin 3 (Fas3) (Fig. 2I,J) were unaffected. The degree of downregulation of each septate junction protein or Gliotactin was insufficient to trigger loss of polarity or to trigger cell death, and we observed no disruption to the epithelium. To test the specificity of the miRNA control, we individually expressed miR-1011 and the miRNA bantam, which are also predicted to target the Gliotactin 3′ UTR (Fig. 1L). Neither miR-1011 nor bantam expression had any effect on Gliotactin (Fig. 2K,L). These results suggest that miR-184 can control Gliotactin and a subset of septate junction mRNAs.

Overexpression of the extracellular domain is the trigger for self-downregulation

The role of miR-184 in Gliotactin control was unexpected because miR-184 mutants are viable with no disc abnormalities (Iovino et al., 2009). Overexpression of Gliotactin is deleterious, leading to cell death, overproliferation and cell migration (Padash-Barmchi et al., 2010), suggesting that mechanisms have evolved to ensure protein levels are tightly controlled. We hypothesized that the overexpression of Gliotactin could trigger elevated miR-184 expression for an additional level of control. To test this hypothesis, we expressed a Gliotactin transgene that lacked the 3′ UTR and in which the intracellular domain had been replaced with a blue fluorescent protein (BFP) tag (Gli::EBFP) (Fig. S1C). With this Gliotactin construct, tyrosine phosphorylation and subsequent endocytosis cannot occur, and endogenous Gliotactin can be analyzed using a monoclonal antibody specific to the intracellular domain. When expressed with the *apterous*-GAL4 driver, Gli::EBFP did not alter the subcellular localization of endogenous Gliotactin nor lead to cell death or disruption of the epithelia, but did result in the overall downregulation of endogenous Gliotactin (Fig. 3A). To confirm these results, we overexpressed a Gliotactin transgene containing the entire protein-coding sequence but lacking the 3′UTR (GliWT) (Fig. S1) in a background with endogenous Gliotactin tagged with YFP (Gli::YFP) (Fig. 3B). Here too, endogenous Gliotactin was downregulated when the transgene was overexpressed. Expression of the Gli::EBFP or GliWT transgenes also led to the downregulation of Mcr and NrxIV (Fig. S2C,D), suggesting that overexpression of Gliotactin leads to

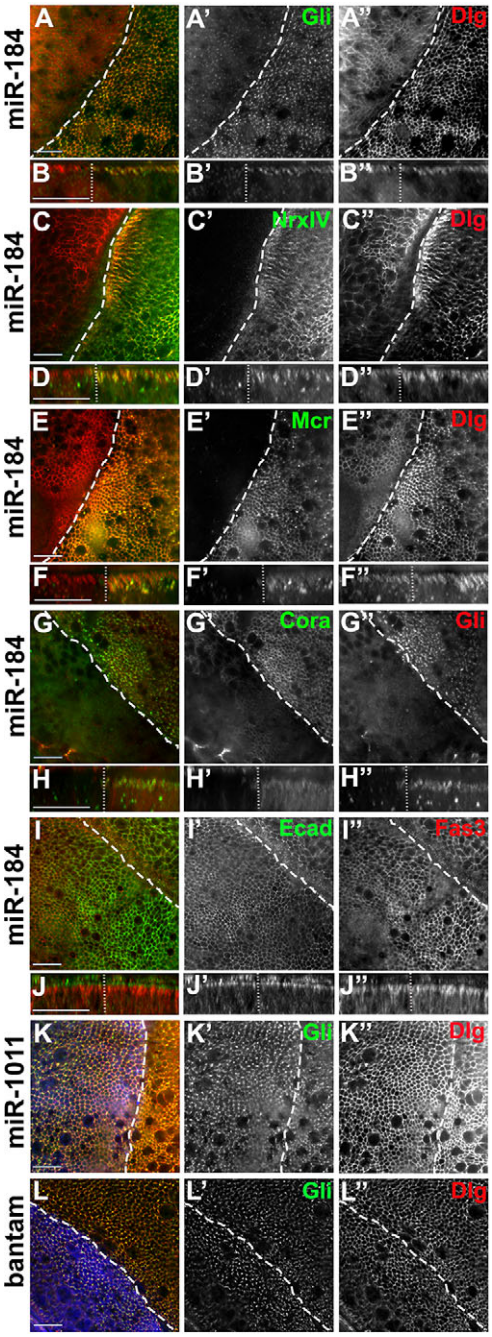

Fig. 2. miR-184 controls a suite of septate junction proteins. In all panels, *apterous*-GAL4 was used to drive expression in the wing disc. The dashed line indicates the dorsal–ventral boundary with the apterous side on the left. (A–J) The expression of miR-184 led to the downregulation of Gliotactin (green, A′), NrxIV (green, C′), Mcr (green, E′) and Coracle (green, Cora, G′) but not Dlg (red, A″–E‴), E-cadherin (green, Ecad, I′) or Fasciclin 3 (red, Fas3, I″). Side projections for each panel are shown below. (K,L) Expression of miR-1011 (K, blue) or bantam miRNA (L, blue) did not reduce the levels of Gliotactin (green,K′,L′) or Dlg (red,K″,L″). All *xy* panels represent a single *z* slice. Scale bars: 15 µm.

Journal of Cell Science (2016) 129, 1477-1489 doi:10.1242/jcs.178608

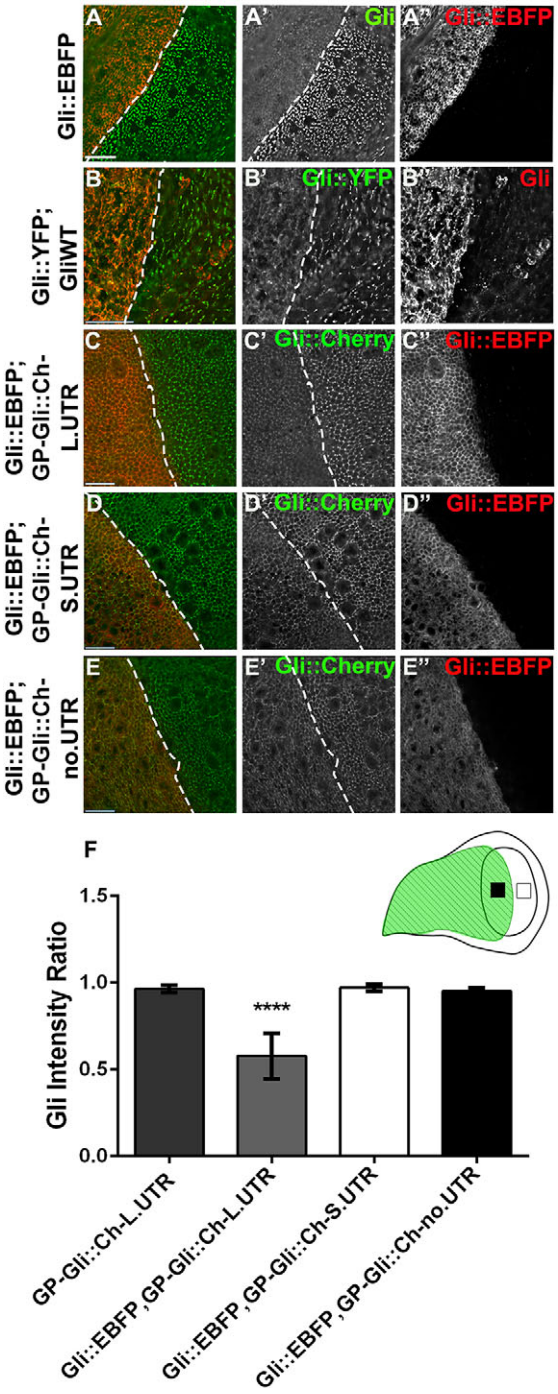

Fig. 3. Gliotactin overexpression triggers self-downregulation through the 3′UTR. *apterous*-GAL4-driven expression in the wing disc. Dashed lines indicate the dorsal–ventral boundary with the apterous side on the left. (A) Expression of Gli::EBFP, lacking the intracellular and 3′UTR domains and tagged with BFP (red, A″), led to downregulation of endogenous Gliotactin (green, A′). (B) Expression of GliWT, a full-length Gliotactin lacking the 3′ UTR (red, B″), caused downregulation of endogenous Gliotactin tagged with YFP (Gli::YFP) (green, B′). (C–E) Expression of Gli::EBFP (red,C″–E″) led to downregulation of GP-Gli::Ch-L.UTR (green, C′) but not of GP-Gli::Ch-S.UTR (green, D′) or GP-Gli::Ch-no.UTR (green, E′). (F) Statistical analysis of the Gliotactin fluorescence intensity on the apterous side (black square in cartoon) normalized to that of the wild-type non-apterous side (white square in cartoon) confirmed that Gli::EBFP significantly downregulated GP-Gli::Ch-L.UTR compared to GP-Gli::Ch-S.UTR or GP-Gli::Ch-no.UTR (n=10 discs, ****P<0.0001, mean±s.d., one-way ANOVA). All panels represent a single z-slice. Scale bars: 15 µm.

elevated miR-184 expression. Overexpression of Gli::EBFP did not downregulate Dlg (data not shown). To determine whether this phenomenon is specific to Gliotactin, we overexpressed NrxIV using an EP insertion in *Nrx-IV* (NrxIV-EP) under the control of *apterous*-GAL4. NrxIV overexpression failed to trigger self-downregulation (Fig. S2A) and failed to downregulate Gliotactin or Mcr (Fig. S2B). These results suggest that the overexpression of the Gliotactin extracellular domain is sufficient to trigger the downregulation of Gliotactin and other septate junction proteins, and that this effect is specific to Gliotactin and not a general property of septate junction proteins.

We next tested to see whether Gli::EBFP triggered downregulation of endogenous Gliotactin through miRNA control of the 3′UTR. To do this, we generated a series of transgenic lines that expressed Cherry-tagged Gliotactin under the control of the *Gliotactin* promoter and with different 3′UTRs: full-length, short and no UTR (Fig. S1B). The *Gliotactin* promoter was used in an attempt to match the normal levels of expression. Each Cherry-tagged protein was trafficked to the TCJ with some spread away from the corners (Fig. S2E–G). When Gli::EBFP was overexpressed in these backgrounds, we observed that only the Gliotactin with the entire 3′UTR (GP-Gli::Ch-L.UTR) was significantly downregulated (Fig. 3C,F). Those with the short 3′ UTR (GP-Gli::Ch-S.UTR) or no 3′UTR (GP-Gli::Ch-no.UTR) were unaffected (Fig. 3D–E) and showed no significant downregulation in protein levels (Fig. 3F). These findings suggest that the overexpression of Gliotactin triggers a feedback loop that specifically targets mRNAs with the long 3′UTR for degradation. Because this region contains the conserved miR-184 recognition sequence, this further indicated that control of Gliotactin mRNA is mediated by miR-184.

Gliotactin mRNA is downregulated and miR-184 increased with Gliotactin overexpression

To confirm that Gliotactin downregulation was at the mRNA level, we used *daughterless*-GAL4 (da-GAL4) to overexpress a full-length Gliotactin with the entire 3′UTR (GliEP) and quantified mRNA levels using RT-PCR analyses (Fig. 4). The EP insertion drives the expression of the endogenous Gliotactin mRNA with the full 3′UTR and, when overexpressed with the strong da-GAL4 driver, Gliotactin mRNA levels were not significantly higher than those of control (Fig. 4A). If there was no miRNA-mediated degradation of the Gliotactin mRNA, we expected to see significantly more Gliotactin mRNA when GliEP was expressed. To test if overexpression of Gliotactin was driving the degradation of endogenous mRNA, we used da-GAL4 to express the Gli::EBFP transgene that lacks the entire intracellular domain and the 3′UTR. Using primers targeted to the intracellular domain, we examined the levels of endogenous Gliotactin mRNA. We found that the mRNA levels for endogenous Gliotactin were reduced compared to those in control when Gli::EBFP was overexpressed (Fig. 4A), confirming that the downregulation of endogenous Gliotactin occurs at the mRNA level.

Our results suggest that Gliotactin mRNA degradation is mediated by miR-184 and that overexpression of Gliotactin leads to an increase in miR-184 levels. To test this hypothesis, we used quantitative real-time (qRT)-PCR to quantify changes in the pre-miR-184 RNA (Enderle et al., 2011). We determined that overexpression of either full-length Gliotactin (GliEP) or Gli::EBFP using *apterous*-GAL4, triggered a significant increase in miR-184 levels compared to those of control (Fig. 4B). Our findings confirmed that induction of miR-184 levels results from

Journal of Cell Science (2016) 129, 1477-1489 doi:10.1242/jcs.178608

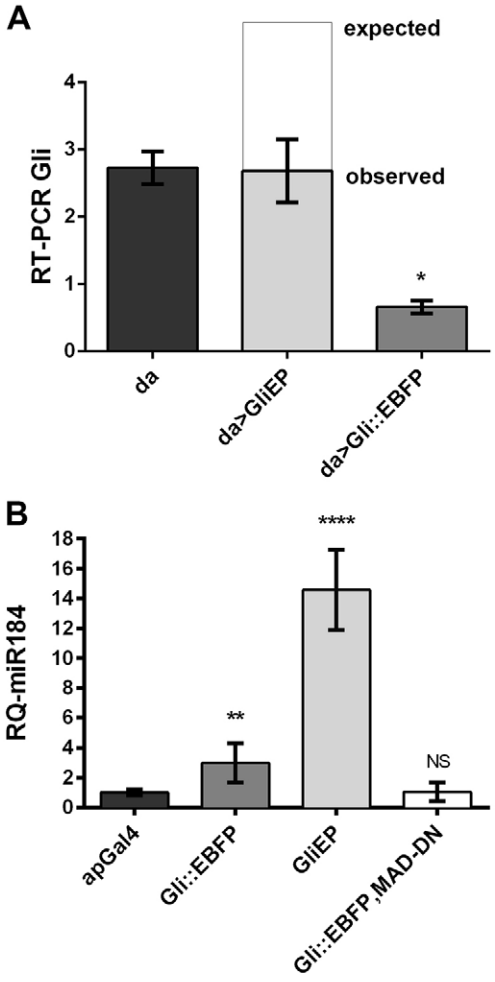

Fig. 4. Gliotactin overexpression leads to reduced Gliotactin mRNA and increased miR-184 expression. (A) RT-PCR analysis of Gliotactin expression in embryos expressing *daughterless*-GAL4 (da-GAL4, da) alone or driving GliEP or Gli::EBFP (da>GliEP and da>Gli::EBFP, respectively). Actin was used as internal control, and the mRNA level of each genotype was normalized against actin level in that genotype (n=3, *P<0.05, one-way ANOVA). (B) qRT-PCR analysis of Gliotactin expression in wing imaginal discs isolated from third instar larvae expressing *apterous*-GAL4 alone (apGal4), or driving either GliEP or Gli::EBFP. miR-184 in GliEP and Gli::EBFP wing discs was significantly higher than that in control (*apterous*-GAL4) (n=8, **P<0.01, ****P<0.0001, one-way ANOVA). Expression of dominant-negative Mad (MAD-DN) with Gli::EBFP blocked the expression of miR-184, and there was no significant (NS) difference compared to the control (n=8, P>0.5, one-way ANOVA). Data are mean±s.d.

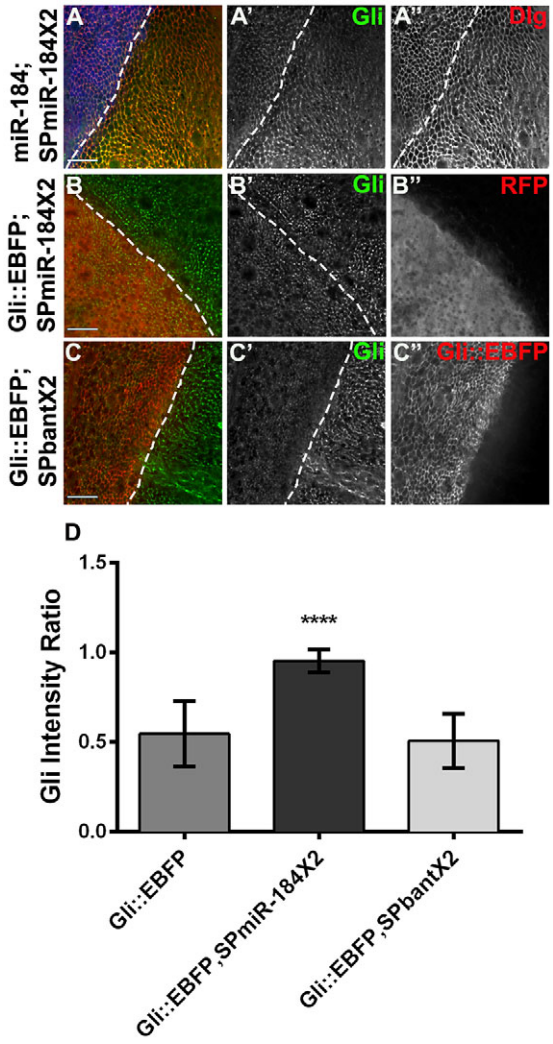

Fig. 5. A miR-184 sponge blocks the Gliotactin downregulation. *apterous*-GAL4-driven expression in the wing disc. Dashed lines indicate the dorsal–ventral boundary, with the apterous side on the left. (A) Co-expression of a miR-184 construct with two copies of the miR-184 sponge (SPmiR-184×2) tagged with mCherry (blue, A) blocked the downregulation of Gliotactin (green, A′). Dlg expression was normal (A″). (B) The miR-184 sponge co-expressed with Gli::EBFP. Two copies of the miR-184 sponge (red, B″) blocked the downregulation of endogenous Gliotactin (green, B′). (C) Co-expression of two copies of a bantam sponge with Gli::EBFP (red, C″). Endogenous Gliotactin (green, C′) was still downregulated. (D) The double miR-184 sponge significantly blocked the downregulation of endogenous Gliotactin (n=10 discs, ****P<0.0001, mean±s.d., one-way ANOVA) relative to the expression of Gli::EBFP alone, whereas the double bantam sponge (SPbant×2) did not. All image panels represent a single z slice. Scale bars: 15 µm.

overexpression of Gliotactin and thereby mediates Gliotactin mRNA levels *in vivo*.

A miR-184 sponge blocks Gliotactin downregulation

As the long 3′UTR of Gliotactin was necessary for the downregulation of the Gliotactin mRNA, this pointed to a role for either miR-184 or miR-1011. We found that miR-184 but not miR-1011 led to the downregulation of Gliotactin and other septate junction proteins (Fig. 2). Next we investigated whether miR-184 was solely responsible. miRNA sponges are an effective means to sequester miRNAs within a cell (Loya et al., 2009). We utilized a sponge specific to miR-184 (SPmiR184) and expressed it using *apterous*-GAL4 within the wing imaginal disc. The sponge alone had no significant effect on endogenous Gliotactin expression (Fig. S2H). However, when two copies of the sponge were expressed along with UAS-miR-184, the downregulation of Gliotactin was blocked (Fig. 5A). To test the effect of the sponge on Gliotactin overexpression, we co-expressed SPmiR-184 with Gli::EBFP and observed that the downregulation of endogenous Gliotactin was blocked (Fig. 5B). To test the specificity of the miRNA, we expressed a bantam sponge (Herranz et al., 2012) along with Gli::EBFP. The bantam sponge did not prevent the downregulation of Gliotactin (Fig. 5C) and the levels of Gliotactin were not significantly different from those in controls expressing Gli::EBFP alone (Fig. 5D). Our findings strongly suggest that miR-184 regulates Gliotactin mRNA levels.

Journal of Cell Science (2016) 129, 1477-1489 doi:10.1242/jcs.178608

miR-184 expression is triggered through the BMP signalling pathway

Our next aim was to determine the mechanism linking overexpression of Gliotactin to the induction of miR-184. miRNA levels are known to be controlled through a number of different pathways, including those involving MAPKs, BMP and TGF-β (Saj and Lai, 2011). There are three MAPKs in *Drosophila melanogaster*, Basket (Bsk; a JNK homologue), p38 (with three isoforms) and rolled (an ERK homologue). We did not observe any changes in the Gli::EBFP-induced reduction of endogenous Gliotactin when Bsk or p38 were blocked using dominant-negative transgenes [Bsk-DN (Petzoldt et al., 2013) and p38-DN (Adachi-Yamada et al., 1999), respectively] or with RNA interference (RNAi)-mediated knockdown of rolled (Biteau and Jasper, 2011) (Fig. S3A–F). These results excluded MAPK signalling as the trigger for miR-184 transcription.

We next tested the role of TGF-β and BMP signalling. Co-expression of Gli::EBFP with dominant-negative Baboon protein (Parker et al., 2006) to block the TGF-β type-I receptor had no effect on the Gli::EBFP-mediated downregulation of Gliotactin (Fig. S3G,H), eliminating possible TGF-β involvement. To block BMP signalling, we co-expressed Gli::EBFP and a dominant-negative form of the BMP type-I receptor, Thickveins (Tkv-DN; Haerry et al., 1998). Expression of dominant-negative Tkv reduced the Gli::EBFP-mediated downregulation of endogenous Gliotactin (Fig. 6A,B,E), whereas dominant-negative Tkv alone had no effect on endogenous Gliotactin levels (nor any additional deleterious effects), suggesting that Tkv was an integral part of the Gliotactin-triggered miR-184 expression.

Ligand activation of Tkv and the type-II BMP receptor Punt leads to the phosphorylation and activation of Mad, a homologue of vertebrate SMAD (Derynck et al., 1996; Newfeld et al., 1996). We observed that expression of Gli::EBFP led to a significant increase in immunolabelling of phosphorylated Mad and to a greater spread of phosphorylated Mad across the dorsal side of the apterous boundary in the wing pouch (Fig. S3I–K). To test whether Mad activation played a role in the miR-184-mediated reduction in Gliotactin levels, we co-expressed Gli::EBFP and a dominant-negative Mad transgene that lacked the DNA-binding domain (Mad-DN; Takaesu et al., 2005). We found that dominant-negative Mad reduced the downregulation of endogenous Gliotactin (Fig. 6C,D,E). Overall blocking of BMP-dependent signalling in conjunction with Gli::EBFP expression significantly inhibited Gliotactin downregulation compared to that with Gli::EBFP alone or with the negative control dominant-negative Bsk (Fig. 6E). To confirm that inhibition of the BMP pathway blocked the increase in miR-184 transcription, we co-expressed Gli::EBFP with dominant-negative Mad and assayed the levels of miR-184 by using qRT-PCR. The level of miR-184 was the same as that in control (*apterous*-GAL4 alone) when the BMP signalling pathway was blocked and was significantly lower than when Gli::EBFP was expressed alone (Fig. 4B). These results suggest that excess Gliotactin triggers an increase in miR-184 through BMP-dependent signalling.

Two further direct tests of the role of Tkv activation in Gliotactin regulation were performed. Activation of Tkv and Mad leads to the induction of transcription of spalt and optomotor blind (omb/bifid) in the wing disc (Blair, 2007). In the first test, we used *omb*-lacZ (Sun et al., 1995) as a reporter of Tkv activation in the presence of increased Gliotactin (Gli::EBFP). We measured the region of *omb*-lacZ induction on the dorsal side compared to that on the ventral side along the *apterous*-GAL4 boundary. The pattern of *omb*-lacZ expression in control discs was evenly matched on both sides of the boundary (Fig. 6F). Overexpression of Gliotactin led to a significant spread of *omb*-lacZ expression on the apterous-dorsal side relative to that on the ventral side (Fig. 6G,H), indicating an increase in Tkv signalling. For the second test, we utilized a fluorescent reporter of Tkv activation (Tkv-TIPF), under the control of UAS, to confirm that the Tkv receptor itself was activated. The Tkv-TIPF reporter emits YFP fluorescence upon receptor activation and displacement of activated FKBP12 (also known as FK506-bp2; Michel et al., 2011). We co-expressed Gli::EBFP with the Tkv-TIPF reporter using *apterous*-GAL4 (Fig. 6J) and compared fluorescence levels to those upon expression of Tkv-TIPF alone (Fig. 6I). Gli::EBFP triggered a significantly higher level of Tkv-TIFP fluorescence compared to that in controls (Fig. 6K). These tests confirm that elevated Gliotactin activates the Tkv receptor, Mad and downstream transcription targets.

Overexpression of Gliotactin activates Tkv signalling through inhibition of Dad

If the BMP receptor mediates the increase in miR-184 transcription, we hypothesized that blocking this pathway enhances the phenotypes observed with overexpression of Gliotactin. Overexpression of Gliotactin with *apterous*-GAL4 leads to the spread of Gliotactin away from the TCJ, resulting in deleterious consequences that include apoptosis, delamination of the columnar epithelia and spread of cells from the dorsal-apterous side into the ventral wild-type side of the wing disc (Fig. 7A) (Padash-Barmchi et al., 2010). When both GliWT and dominant-negative Tkv were co-expressed in the wing imaginal disc, we observed that blocking Tkv signalling significantly enhanced the spread of the Gliotactin-overexpressing cells into the ventral half of the disc (Fig. 7B,E). However, when both GliWT and an activated form of Tkv (Tkv-Act) were co-expressed, we observed that increased Tkv activation completely blocked the cell migration (Fig. 7C,E). When GliWT was co-expressed with the miR-184 sponge, this increased migration of the Gliotactin-overexpressing cells (Fig. 7C,E). However, simultaneous expression of Gliotactin and miR-184 significantly reduced the cell migration (Fig. 7I,E). Taken together, these results show that loss of Tkv signalling and block of miR-184 lead to increased levels of endogenous Gliotactin expression and enhance the deleterious effects resulting from Gliotactin overexpression. Increased Tkv signalling and miR-184 expression suppressed the Gliotactin phenotypes.

We next wanted to establish the mechanism by which increased Gliotactin leads to activation of Tkv. To determine whether Tkv activation is through the ligand Deacapentaplegic (Dpp), GliWT and Dpp (UAS-Dpp::GFP) (Teleman and Cohen, 2000) were co-expressed in the wing imaginal disc. An increase in Dpp did not block the migration of cells overexpressing Gliotactin into the ventral half of the disc (Fig. 7F arrow, J). In control discs, the overexpression of Dpp::GFP, driven by *apterous*-GAL4, had no effect on endogenous Gliotactin expression (data not shown; n=10 discs). Therefore, increased Dpp expression was not the cause of increased Tkv activation by Gliotactin. An alternative route to activation of Tkv could be through inhibition of Dad, a Tkv inhibitor. We expressed GliWT in a *Dad* heterozygous mutant ($Dad^{[j1E4]/+}$), which completely blocked the migration of GliWT cells into the ventral side of the disc (Fig. 7G,J). Co-expression of GliWT and an EP (UAS) insertion in *Dad* (DadEP), to increase Dad expression, resulted in enhanced cell migration (Fig. 7H, arrow and J). These results suggest that the activation of Tkv by Gliotactin is through

Journal of Cell Science (2016) 129, 1477-1489 doi:10.1242/jcs.178608

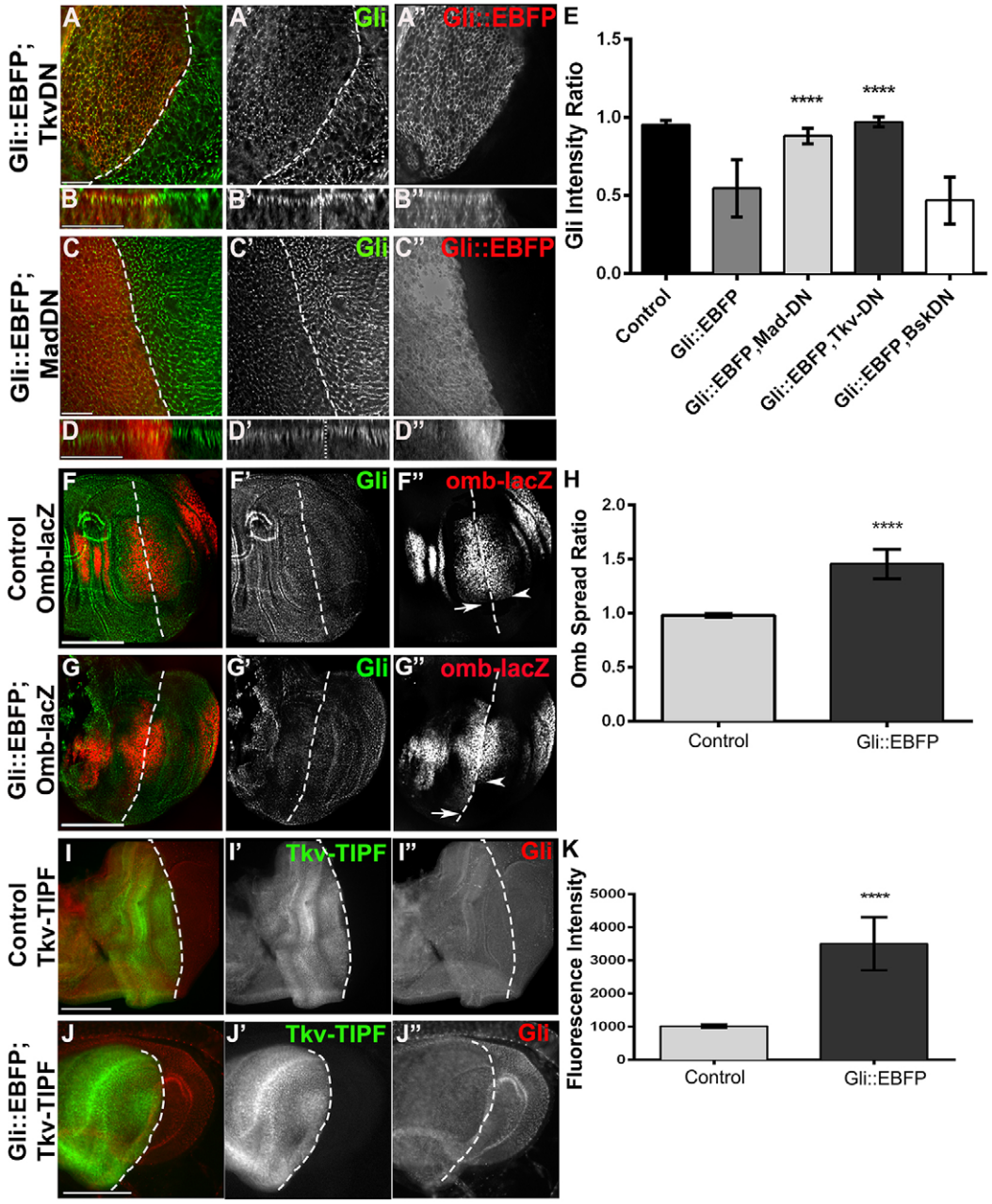

Fig. 6. BMP receptor Tkv signalling is key to Gliotactin regulation. *apterous*-GAL4-driven expression in the wing disc. Dashed lines indicate the dorsal–ventral boundary with the apterous side on the left. Side projections are shown for each corresponding *xy* panel in A and C. (A–D) Co-expression of Gli::EBFP (red, A″-D″) with dominant-negative Tkv (Tkv-DN, A) or dominant-negative Mad (MAD-DN, C) blocked the downregulation of endogenous Gliotactin (green, A′-D′). B and D show side views. (E) The block in downregulation of endogenous Gliotactin by Tkv-DN and Mad-DN was significant when compared to that upon expression of Gli::EBFP alone (n=10 discs, ****P<0.0001, mean±s.d., one-way ANOVA). In contrast, dominant-negative Basket (Bsk-DN) had no effect on Gliotactin downregulation. (F) Expression of omb-lacZ (red, F″) in a control disc. omb-lacZ expression spanned the dorsal–ventral boundary (arrow dorsal and arrowhead ventral), with equal distribution on either side. (G) Expression of Gli::EBFP (green, G′) triggered the spread of omb-lacZ (red, G″) along the dorsal–ventral boundary on the apterous side (arrow dorsal and arrowhead ventral). (H) The region of omb-lacZ expression was significantly greater with GliWT compared to wild type (n=10 discs, ****P<0.0001, mean±s.d., one-way ANOVA). (I–K) Comparison of the fluorescence intensity of Tkv-TIPF (green, I′, J′) alone or co-expressed with Gli::EBFP shows increased activation of Tkv by Gli::EBFP. Gliotactin immunolabeling (red, I″, J″). (K) Quantification confirmed a significant increase in the fluorescence intensity of Gli::EBFP with Tkv-TIPF compared to Tkv-TIPF alone (n=10 discs, ****P<0.0001, mean±s.d., t-test). (A–D) All *xy* panels represent a single *z* slice. Scale bars: 15 µm. Scale bars: 50 µm (F–J).

inhibition of Dad. Our combined results indicate that the feedback loop to control Gliotactin mRNA works through activation of the BMP signalling pathway (Fig. 8). Activation occurs through inhibition of Dad, resulting in increased Tkv receptor signalling and phosphorylation of Mad, leading to increased transcription of miR-184.

DISCUSSION

Gliotactin, a TCJ protein, is crucial for the formation of septate junctions, the TCJ and the function of permeability barriers. At the protein level, Gliotactin is tightly controlled by tyrosine phosphorylation and endocytosis, and overexpression of Gliotactin leads to spread beyond the TCJ, with deleterious

Journal of Cell Science (2016) 129, 1477-1489 doi:10.1242/jcs.178608

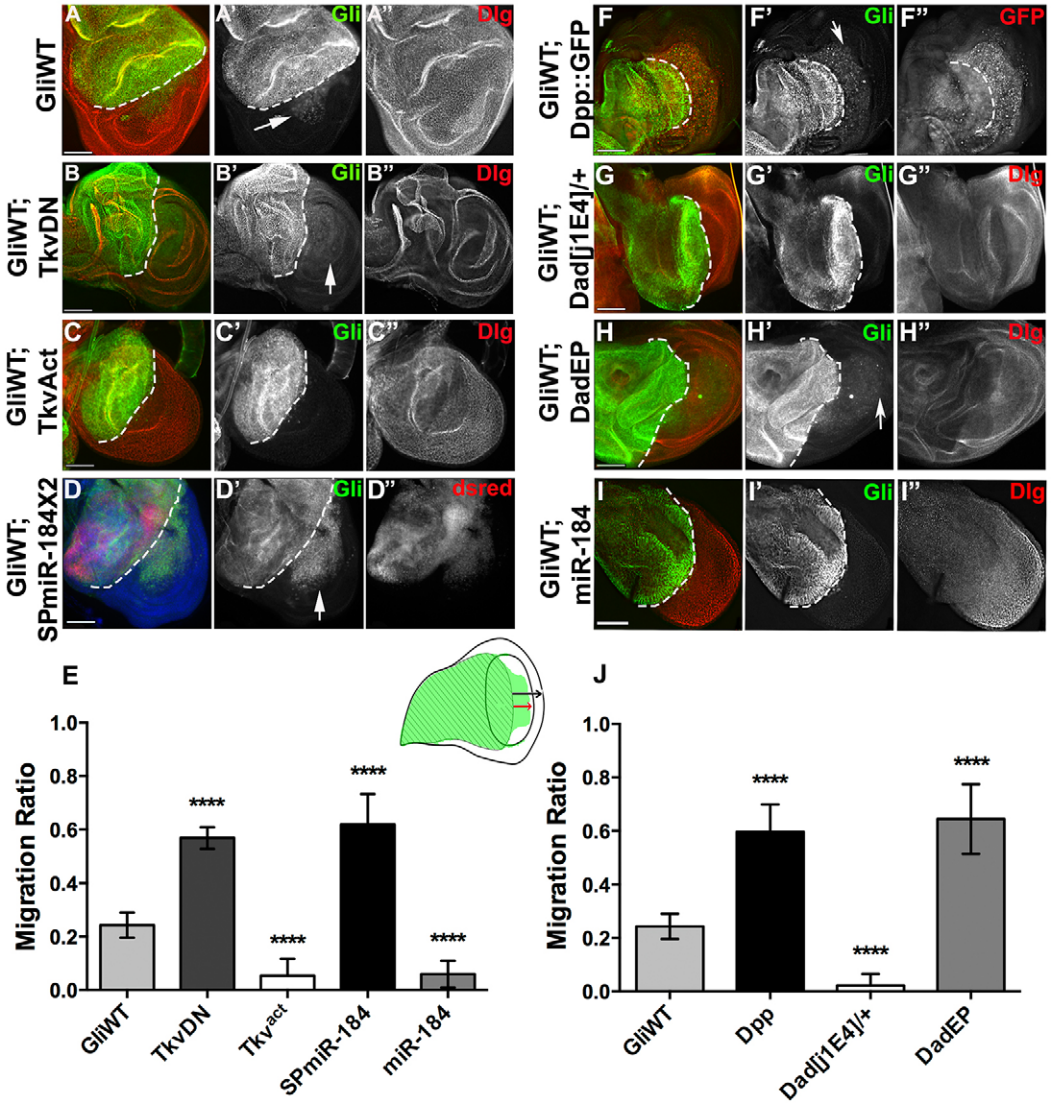

Fig. 7. Gliotactin phenotypes can be enhanced or suppressed by changing Tkv signalling levels. *apterous*-GAL4-driven expression in the wing imaginal disc. The dashed line indicates the dorsal–ventral boundary with the apterous side on the left. (A) Overexpression of GliWT (green, A′) triggered apoptosis and the migration of delaminated cells into the non-apterous (ventral) side of the disc (arrow) (Dlg, red, A″). (B) Co-expression of GliWT (green, B′) and a dominant-negative Tkv construct (Tkv-DN) increased the migration of cells into the non-apterous side of the disc (arrow) (Dlg, red, B″). (C) Co-expression of GliWT (green, C′) and activated Tkv (Tkv-Act) blocked the spread of cells (Dlg, red, C″). (D) Co-expression of GliWT (green, D′) and two copies of the miR-184 sponge (SPmiR-184X2, red, D″) increased cell migration and enhanced the effects of Gliotactin overexpression. (E) The degree of migration was quantified as illustrated in the wing disc cartoon. The distance that GliWT cells migrated from the apterous into the non-apterous side (red arrow) was compared to the distance from the apterous boundary to the distal wing edge (black arrow). For A–D,I, co-expression of Tkv-DN or the miR-184 sponge (SPmiR-184) significantly increased the migration of GliWT cells, whereas co-expression of Tkv-Act (Tkv^{act}) or miR-184 significantly decreased migration. (For all: n=10 discs, ****P<0.0001, mean±s.d., one-way ANOVA.) (F) Co-expression of GliWT (green, F′) and Dpp::GFP (red, F″) enhanced cell migration. (G) Expression of GliWT (green, G′) in a heterozygous Dad mutant (*Dad[j1E4]*/+) blocked migration (Dlg, red, G″). (H) Co-expression of GliWT (green, H′) with an EP insertion in *Dad* (DadEP) to increase Dad expression enhanced migration of Gliotactin-expressing cells (Dlg, red, H″). (I) Co-expression of GliWT (green, I′) and miR-184 prevented the migration of GliWT cells (Dlg, red, I″). (J) The degree of migration in F–H was quantified. Cell migration in GliWT-, Dpp::GFP- and GliWT-, DadEP-expressing wings was significantly increased, whereas migration in GliWT, *Dad[j1E4]*/+ was significantly decreased compared to GliWT alone. (For all: n=10 discs, ****P<0.0001, mean±s.d., one-way ANOVA) Scale bars: 50 µm.

consequences including delamination, cell migration and apoptosis (Padash-Barmchi et al., 2010). We found that Gliotactin is also regulated at the mRNA level, specifically by miR-184-mediated degradation through a conserved miR-184-target site in the 3′UTR. Furthermore, we demonstrate that miR-184 controls other septate junction proteins, including NrxIV, Coracle and Mcr. We propose that excessive Gliotactin acts as the trigger to induce miR-184 expression through the activation of BMP signalling and the Tkv type-I BMP receptor. Activation of Tkv is not through elevated levels of its ligand Dpp, but through inhibition of Dad, an inhibitory SMAD.

Gliotactin overexpression acts as the trigger for miR-184 induction

miR-184 is expressed throughout *Drosophila* embryogenesis in the brain, ventral nerve cord (Li et al., 2011), mesoderm, endoderm (Aboobaker et al., 2005) and in imaginal discs at larval stages (Li et al., 2011). miR-184 regulates germline development, where loss

Journal of Cell Science (2016) 129, 1477-1489 doi:10.1242/jcs.178608

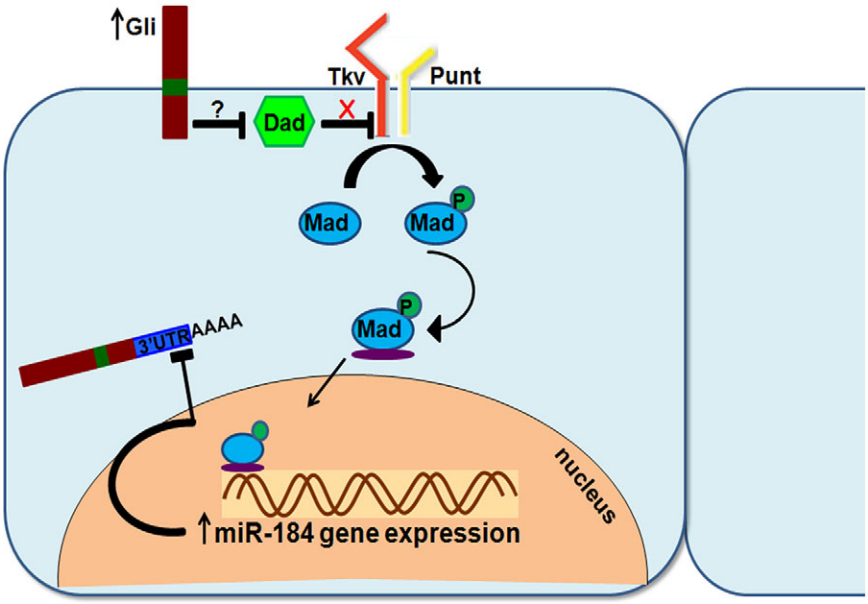

Fig. 8. Gliotactin auto-regulation model. Increased Gliotactin expression leads to the dissociation of Dad from Tkv, resulting in increased Tkv activation and increased phosphorylation of Mad. Activated Mad leads to increased miR-184 transcription, which in turn binds to target sequences on the 3′UTR of Gliotactin and reduces Gliotactin mRNA levels. P, phosphorylation.

of miR-184 leads to oogenesis defects (Iovino et al., 2009). However, *miR-184* null mutants are viable with normal morphology, leading to the suggestion that maternally deposited miR-184 might persist through embryogenesis, allowing development into larval stages and beyond (Iovino et al., 2009). An alternative explanation is that miR-184 is expressed at basal levels throughout development, but increased expression and function occurs through a trigger. Our findings suggest that overexpression of Gliotactin is a trigger for increased miR-184 transcription and that this in turn leads to the downregulation of a suite of other septate junction proteins. *In vitro* luciferase assays have previously identified Gliotactin, NrxIV, Contactin, Coracle, Megatrachea, Sinuous and Kune-Kune as potential targets of miR-184 (Kertesz et al., 2007). Our *in vivo* results show that miR-184 regulates Gliotactin at the mRNA level as part of a feedback loop.

miRNAs play a key role in the regulation and maintenance of a range of vertebrate epithelia. For instance, miR-200 is enriched in breast and ovarian epithelia, and can suppress the epithelia-to-mesenchymal transition (Gregory et al., 2008; Park et al., 2008). miR-122a regulates intestinal tight junction permeability by targeting Occludin mRNA (Ye et al., 2011). miR-184 is expressed at high levels in the vertebrate eye, including the retina pigmented epithelia, cornea and lens (Kapsimali et al., 2007; Ryan et al., 2006), and regulates the blood–retina barrier (Wang et al., 2010) as well as angiogenesis (Yu et al., 2008). Collectively, these findings reveal a role of miRNAs in the control and maintenance of epithelial cells.

In the *Drosophila* imaginal disc, miR-184 controls the levels of a suite of septate junction proteins and the TCJ protein Gliotactin. During imaginal disc development, there is a dynamic reorganization of the septate junctions as cells rearrange to generate the structures of the adult wing (Fristrom, 1982). Intact septa either become extended or compacted in response to these cellular movements in order to maintain the transepithelial barrier. Thus, miR-184 might function to coordinate septate junction domain proteins during imaginal epithelial morphogenesis to ensure that cells move and rearrange more easily as the wing structures develop. However, expression of the miR-184 sponge did not generate defects in wing morphogenesis, and *mir-184* mutants are viable with no defects in epithelial morphogenesis, suggesting that increased miR-184 expression is transient and localized. Because the septate junction complex is highly stable (Oshima and Fehon, 2011), it is likely that basal levels of miR-184 have little impact on the septate junction domain. Rather, a localized increase in miR-184 in response to a trigger would be necessary to change the stability of this complex, as might occur during dynamic processes such as morphogenesis, proliferation, migration or apoptosis. miRNAs in both *Drosophila* and vertebrates can regulate apoptosis by controlling the levels of pro-apoptotic or anti-apoptotic genes (Jovanovic and Hengartner, 2006). For instance, the *Drosophila* death genes Drice, hid, reaper, grim and sickle are targeted either individually or as a group by miRNAs, including miR-2, miR-6, miR-2/13, miR-11, miR-14 and miR-308 (Leaman et al., 2005; Stark et al., 2003; Xu et al., 2003). In particular, the bantam miRNA promotes cell proliferation through regulation of hid (Brennecke et al., 2003) and is controlled by the Dpp pathway (Martín et al., 2004; Doumpas et al., 2013; Oh and Irvine, 2011; Zhang et al., 2013). Thus, an increase in miR-184 might be triggered by Tkv activation during the processes that underlie the apoptosis stimulated by overexpression of Gliotactin.

BMP signalling pathway induces miR-184 activation

Our analysis points to the BMP signalling pathway as part of the miR-184 trigger downstream of Gliotactin overexpression. In vertebrates, BMP or TGF-β signalling pathways play an important role in the transcription and biogenesis of miRNAs (Kato et al., 2009; Winbanks et al., 2011). BMP4 and TGF-β elevate the levels of 20 different species of miRNAs and recruit receptor-regulated SMADs (R-Smads) to enhance Drosha processing of pri-miRNAs (Davis et al., 2008; Harris and Ashe, 2011; Saj and Lai, 2011). BMP control of microRNA biogenesis and processing has been shown to control the proliferation and maintenance of vertebrate epithelia (Saj and Lai, 2011; Wang et al., 2010). For instance, TGF-β activation of miR-204 and miR-211 (miR-204/211) leads to targeting of SNAIL2, which normally represses Claudin transcription and other proteins crucial for maintaining epithelial structure (Carrozzino et al., 2005). miR-204 in retinal pigment epithelium inhibits TGF-βR2, Smad3 and SNAIL1 and SNAIL2 to protect tight junction integrity (Wang et al., 2010). These findings suggest that the expression of miR-204/

Journal of Cell Science (2016) 129, 1477-1489 doi:10.1242/jcs.178608

211 and involvement of TGF-β signalling in a feedback loop is an important signal for integrity and maintenance of tight junctions (Kato et al., 2009; Xu et al., 2009).

In *Drosophila*, Dpp signalling and Mad can control cell proliferation through transcriptional control of the bantam microRNA through different transcription factors, including omb, brinker and yorkie (Martín et al., 2004; Doumpas et al., 2013; Oh and Irvine, 2011; Zhang et al., 2013). Our data show that overexpression of Gliotactin elevated Mad phosphorylation and increased transcription of omb, but we found no evidence that the bantam miRNA was involved in Gliotactin or septate junction protein control. The predicted bantam-targeted site was retained within the short *Gliotactin* 3′UTR, and neither the expression of bantam miRNA nor the bantam sponge had an effect on Gliotactin levels.

We propose that Gliotactin activates the BMP signalling pathway to increase pri-miR-184 transcription, acting through Tkv and Mad. Co-expression of Gliotactin with dominant-negative Mad blocked the increase in transcription of miR-184 and prevented the resulting downregulation of endogenous Gliotactin. It is likely that Gliotactin acts upstream of Mad through activation of the Tkv receptor. The increased fluorescence intensity of the Tkv-TIPF reporter upon Gliotactin overexpression confirms that the Tkv receptor itself is activated in response to overexpression of Gliotactin, either indirectly or directly. Gliotactin might increase the BMP ligand–receptor interaction, perhaps through increased membrane retention, increased ligand levels or increased capacity for ligand–receptor interactions. Alternatively, Gliotactin might interfere with an inhibitor of Tkv, such as the inhibitory Smad Dad. Dad is stably associated with Tkv and negatively regulates phosphorylation of Mad, probably by competing with Mad for Tkv binding (Bokel et al., 2006; Inoue et al., 1998). Our results favour the latter explanation, that Gliotactin increases Tkv signalling through disruption of Dad. Increased Dpp expression did not rescue the effects of overexpressed Gliotactin in the wing disc. Conversely, a reduction of the *Dad* gene dose by 50% completely suppressed the Gliotactin overexpression phenotypes, whereas increased Dad expression enhanced those phenotypes. These results point to a feedback loop by which Gliotactin reduces the association of Tkv and Dad to increase Tkv activation. Whether this interaction is intra- or extracellular, or indirect remains to be determined. Gliotactin interacts with the MAGUK scaffolding protein Dlg (Padash-Barmchi et al., 2010); however, the signalling complex formed between Gliotactin and Dlg is mediated by the PDZ-binding motif (Padash-Barmchi et al., 2013). Because Gli::EBFP lacks this domain, it is unlikely that the activation of miR-184 is mediated by the binding of a PDZ protein. Rather, the extracellular domain is likely to mediate the interactions that trigger Tkv activation. However, if there are other triggers of Tkv and miR-184 production, these have yet to be determined.

The activation of Mad by Tkv leading to increased miR-184 expression could be due to the direct transcriptional activation of miR-184 by Mad, or through the removal of an inhibitor such as brinker. The growth-promoting function of Dpp works through the repression of the transcription-repressor brinker (Schwank et al., 2008). Over 1000 genes have been identified as potential brinker targets, including the bantam miRNA (Doumpas et al., 2013; Oh and Irvine, 2011). However, miR-184 has not been identified as a brinker target. Regardless of the transcription mechanism, our model proposes that increased Gliotactin leads to displacement of Dad from Tkv, increased Mad activation and miR-184 transcription, which reduces Gliotactin mRNA levels within the cell. Thus, Gliotactin is subject to two levels of regulation – at the protein level through tyrosine-mediated phosphorylation and endocytosis and at the mRNA level through miR-184 mediated-degradation that is stimulated by Tkv receptor signalling.

MATERIALS AND METHODS

Fly stocks

The following fly strains were used: Gli$^{[EP2306]}$, NrxIV$^{[EP604]}$ (Rorth, 1996), UAS-GliWT (Schulte et al., 2006), Gli::YFP (Kyoto DGRC), NrxIV::GFP (Buszczak et al., 2007), UAS-mCD8::RFP (Bloomington), UAS-miR-184 (Iovino et al., 2009), UAS-miR-1011(Bejarano et al., 2012), UAS-sponge-bantam (Herranz et al., 2012), UAS-bantam (Yang et al., 2008), UAS-Bsk-DN (Petzoldt et al., 2013), UAS-p38-DN (Adachi-Yamada et al., 1999), UAS-rolled-RNAi (Biteau and Jasper, 2011), UAS-Tkv-Act (Haerry et al., 1998) and UAS-Tkv-DN (Haerry et al., 1998), UAS-Tkv-TIPF (Michel et al., 2011), UAS-Mad-DN (Takaesu et al., 2005), UAS-Baboon-DN (Parker et al., 2006), UAS-Dpp::GFP (Teleman and Cohen, 2000), *Dad$^{[j1E4]}$* (Ogiso et al., 2011), Dad$^{[EP3196]}$ (Bellen et al., 2004), omb-lacZ (Sun et al., 1995) and *apterous*–GAL4 (Bloomington *Drosophila* Stock Center).

Generation of transgenic lines

For the generation of the *Gliotactin* 3′UTR transgenic lines, the entire coding sequence of Gliotactin was amplified from a Gliotactin cDNA (AE27.41) (Auld et al., 1995). The Gliotactin coding sequence, an mCherry tag and one of three different UTRs [no 3′UTR (SV40), short 3′UTR (AE27.41, Auld et al., 1995) and long 3′UTR (RE15719, *Drosophila* Genomics Resource Center)] were amplified using the following primers: extracellular-Gliotactin5: 5′-TCTAGATCATCATGATGCAC-3′ (*Xba*I site) and extracellular-Gliotactin3: 5′-GAATTCCAGGGTCAACGAATC-3′ (*Eco*RI site); mCherry5: 5′-GAATTCATGGTGAGCAAGGGAGAG-3′ (*Eco*RI site) and mCherry3: 5′-AAGCTTCTTGTACAGCTCGTCCATG-3′ (*Hind*III site); Gliotactin-transmembrane5: 5′-AAGCTTGATGTATTCG-TGACCAC-3′ (*Hind*III site) and Gliotactin-transmembrane3: 5′-CGTAC-GCCACATGATGCAGCAGATG-3′ (*Bsi*WI); C-terminal-Gliotactin5: 5′-CGTACGCGCAATGCCAAGCGCCAATC-3′ (*Bsi*WI site) and C-terminal-Gliotactin3: 5′-GACGTCTTATACGGATGTCTGAGGCAC-3′; no-3′UTR (SV40)5: 5′-GACGTCGATCTTTGTGAAGGAAC-3′ (*Aat*II site) and no-3′UTR (SV40) 3: 5′-CTCGAGGATCCAGACATGATAAGA-3′(*Xho*I site); short-3′UTR5: 5′-GACGTCGTAACAGCTCTCTAAGCG-CAG-3′ (*Aat*II site) and short-3′UTR3: 5′-CTCGAGTTTGTTATCAAA-TAATAGCAG-3′ (*Xho*I site); long-3′UTR5: 5′-GACGTCGTAACAGCT-CTCTAAGCGCAG-3′ (*Aat*II site) and long-3′UTR3: 5′-CTCGAGATA-TTTATTTATGGACAAATACATAAAAC-3′ (*Xho*I site).

The Gliotactin promoter was amplified using the following primers: Gliotactin-promoter5: 5′-CACTTGGATCCTTATTTACAATCA-GC-3′ (*Bam*HI site) and Gliotactin-promoter3: 5′-GATGATCTAGAAA-AATATTCAAAAGTAG-3′ (*Xba*I site).

PCR products were subcloned into the pβSΔF′ vector and sequenced for verification. The UTR constructs (no, short and long 3′UTR) were subcloned into pUAST-linker vector or 3′ to the Gliotactin promoter (3.7 Kb) in the pCasper 5 vector. To generate the pUAS-Gli::EBFP line, the enhanced BFP (Addgene) was PCR amplified and introduced into the GliNter construct, as previously described (Padash-Barmchi et al., 2010) using the *Spe*I and *Eco*RI restriction sites. Each construct was sequenced, and multiple independent transgenic lines were generated (Genetic Services).

The miR-184 sponge (SPmiR-184) construct contains 20 repetitive seed complementary sequences separated by variable four-nucleotide linkers, assembled as previously described (Loya et al., 2009) and cloned into the 3′ UTR of mCherry between *Not*I and *Xba*I sites in a modified pWALIUM10-moe vector (Ni et al., 2009), carrying the white+ marker and flanking insulator sequences (Bejarano et al., 2012); the combined miRNA and linker sequences were checked against every mature miRNA sequence in the *Drosophila* genome to prevent off-target effects. Transgenic strains were generated using phiC31 site-specific genomic integration on the second (*attP40*) and third (*attP2*) *Drosophila* autosomes (Genetic Services).

RNA analysis

Reverse transcriptase PCR

Embryos were collected and dechorionated in 50% bleach. Total RNA was extracted using Trizol (Invitrogen). 2 µg of total mRNA was used to synthesize the cDNA using random hexamers and Superscript II reverse transcriptase (Applied Biosystems). Synthesized cDNA was amplified using AE2XI and AE2XII primers from the C-terminus of Gliotactin. AE2XI primer: 5′-GCGTGGAGTGGACAATGCCC-3′; AE2XII primer: 5′-GGAATTCCGCTGACTCCCTAAGCGCATCC-3′. Actin primers were used as an internal control. The expression data were normalized to the levels of actin. Band intensity was measured using ImageJ, and data were analyzed using one-way ANOVA and GraphPad Prism6.

qRT-PCR

RNA was extracted from 60 third instar wing discs, and RNA was extracted using QIAGENE RNeasy kit. 1 µg of total RNA was used to generate cDNA with random primers and Superscript III reverse transcriptase (Applied Biosystems). SYBR GREEN-based qRT-PCR (Bio-Rad) was performed for miR-184 and actin. qRT-PCR conditions were used for *apterous*-GAL4, GliEP, Gli::EBFP and Mad-DN lines using primers designed for pre-miR-184 (Enderle et al., 2011). Forward primer sequence: 5′-ATGCACATGAGTTGGCAGACAGC-3′, reverse primer sequence: 5′-CTTACCCCACGTTTCGATTACGC-3′. qRT-PCR cycling conditions were 95°C for 30 s, 40× (95°C for 5 s, 60°C for 30 s). qRT-PCR data were analyzed by using the comparative ΔΔCt method (Livak and Schmittgen, 2001). qRT-PCR products were sequenced to confirm primer specificity.

Statistical analyses

All statistical tests were calculated and graphed with GraphPad Prism 6. Immunofluorescence levels were quantified using ImageJ (Schneider et al., 2012). Fluorescence intensity of UAS-Gli::Ch constructs was measured across two areas on the apterous side (Fig. 1J). The intensity ratio was calculated, and significance was calculated using a one-way ANOVA with Tukey's post-hoc test. For all other figures, the mean intensity was calculated using the same fixed-size square in the pouch region of the apterous and the wild-type sides of wing imaginal disc (Fig. 3). The ratio of intensity in the apterous side compared to intensity in the wild-type side was calculated. The migration of Gliotactin-overexpressing cells (Fig. 7) from the apterous side into the wild-type side of the wing imaginal disc was measured, and the distance of spread was calculated as a ratio of the length of the ventral, or wild-type, side of the disc. Significance was determined using a one-way ANOVA with Tukey's post-hoc test.

For Tkv-TIPF quantification (Fig. 6I,J), fluorescence intensity was measured in a set area with ImageJ on the apterous side with or without Gli::EBFP. Discs from both genotypes were analyzed at the same time, images were collected with the same exposure time and neutral density filters, and were deconvolved using the same protocol. Significance was determined using an unpaired *t*-test.

Immunolabelling

Third instar larval imaginal discs were stained as described previously (Schulte et al., 2006). Primary antibodies were: mouse anti-Gli 1F6.3 at 1:200 (Auld et al., 1995), rabbit anti-Gli at 1:300 (Venema et al., 2004), mouse anti-Dlg 4F3 at 1:200 (Developmental Studies Hybridoma Bank) (Parnas et al., 2001), rat anti-DE-Cadherin at 1:50 (Developmental Studies Hybridoma Bank), mouse anti-Coracle (9C and C615-16B cocktail) at 1:100 (Developmental Studies Hybridoma Bank) (Fehon et al., 1994), rabbit anti-NrxIV at 1:500 (Baumgartner et al., 1996), guinea pig anti-Mcr at 1:800 (Hall et al., 2014), mouse anti-Fasciclin 3 at 1:100 (Developmental Studies Hybridoma Bank), rabbit anti-phosphorylated Mad at 1:200 (Cell Signaling). DAPI was used at 1:1000 (Thermo Scientific). Secondary antibodies were used at 1:300 – goat anti-rabbit (conjugated to Alexa Fluor 647 or Alexa Fluor 568), goat anti-mouse (conjugated to Alexa Fluor 647, Alexa Fluor 488 or Alexa Fluor 568), goat anti-rat (conjugated to Alexa Fluor 647 or Alexa Fluor 568) (Molecular Probes).

Imaging

Image stacks were collected with a DeltaVision Spectris microscope (Applied Precision, Issaquah, WA) with a 20× air- or 60× oil-immersion lens (NA1.4) and CoolSnap HQ digital camera. Deconvolution of 0.2 m *z*-sections with SoftWorx (Applied Precision) used a point-spread function measured from 0.2-µm beads conjugated with Alexa dyes (Molecular Probes) mounted in Vectashield (Vector Labs). Side projections were created using the SoftWorx program. Images were exported to Photoshop (Adobe Systems) for compilation.

Acknowledgements

We thank Dr Doug Allan (University of British Columbia, Vancouver, Canada) for providing antibodies; Drs Steve Cohen (University of Copenhagen, Copenhagen, Denmark), Issac Edery (Rutgers University, Piscataway, NJ) and Doug Allan, and the Bloomington and *Drosophila* Genomics Resource Centers for fly stocks; the TRiP at Harvard Medical School (National Institutes of Health - National Institute of General Medical Sciences R01-GM084947) for providing transgenic RNAi fly stocks. The monoclonal antibodies listed from the Developmental Studies Hybridoma Bank were developed under the auspices of the The Eunice Kennedy Shriver National Institute of Child Health and Human Development and maintained by The University of Iowa, Department of Biology. We also thank Dr Doug Allan for helpful discussions and comments on the manuscript.

Competing interests

The authors declare no competing or financial interests.

Author contributions

Z.S. contributed to all aspects of the manuscript, including writing and editing of the manuscript, study design, data collection, analysis and interpretation. M.P.-B., M.M.G. and G.S. contributed data collection, analysis and to the editing of the manuscript. T.A.F. and D.V.V. contributed unpublished reagents, and D.V.V. contributed to editing of the manuscript. V.J.A. contributed study conception and design, data interpretation, writing, and editing of the manuscript.

Funding

This study was supported by the Canadian Institutes for Health Research [MOP-123420 to V.J.A.] and the National Institute of Neurological Disorders and Stroke [R01 NS069695 to D.V.V.]. Deposited in PMC for release after 12 months.

Supplementary information

Supplementary information available online at
http://jcs.biologists.org/lookup/suppl/doi:10.1242/jcs.178608/-/DC1

References

Aboobaker, A. A., Tomancak, P., Patel, N., Rubin, G. M. and Lai, E. C. (2005). Drosophila microRNAs exhibit diverse spatial expression patterns during embryonic development. *Proc. Natl. Acad. Sci. USA* **102**, 18017-18022.

Adachi-Yamada, T., Nakamura, M., Irie, K., Tomoyasu, Y., Sano, Y., Mori, E., Goto, S., Ueno, N., Nishida, Y. and Matsumoto, K. (1999). p38 mitogen-activated protein kinase can be involved in transforming growth factor beta superfamily signal transduction in Drosophila wing morphogenesis. *Mol. Cell. Biol.* **19**, 2322-2329.

Auld, V. J., Fetter, R. D., Broadie, K. and Goodman, C. S. (1995). Gliotactin, a novel transmembrane protein on peripheral glia, is required to form the blood-nerve barrier in Drosophila. *Cell* **81**, 757-767.

Batz, T., Forster, D. and Luschnig, S. (2014). The transmembrane protein Macroglobulin complement-related is essential for septate junction formation and epithelial barrier function in Drosophila. *Development* **141**, 899-908.

Baumgartner, S., Littleton, J. T., Broadie, K., Bhat, M. A., Harbecke, R., Lengyel, J. A., Chiquet-Ehrismann, R., Prokop, A. and Bellen, H. J. (1996). A Drosophila neurexin is required for septate junction and blood-nerve barrier formation and function. *Cell* **87**, 1059-1068.

Bejarano, F., Bortolamiol-Becet, D., Dai, Q., Sun, K., Saj, A., Chou, Y.-T., Raleigh, D. R., Kim, K., Ni, J.-Q., Duan, H. et al. (2012). A genome-wide transgenic resource for conditional expression of Drosophila microRNAs. *Development* **139**, 2821-2831.

Bellen, H. J., Levis, R. W., Liao, G., He, Y., Carlson, J. W., Tsang, G., Evans-Holm, M., Hiesinger, P. R., Schulze, K. L., Rubin, G. M. et al. (2004). The BDGP gene disruption project: single transposon insertions associated with 40% of Drosophila genes. *Genetics* **167**, 761-781.

Biteau, B. and Jasper, H. (2011). EGF signaling regulates the proliferation of intestinal stem cells in Drosophila. *Development* **138**, 1045-1055.

Blair, S. S. (2007). Wing vein patterning in Drosophila and the analysis of intercellular signaling. *Annu. Rev. Cell Dev. Biol.* **23**, 293-319.

Bokel, C., Schwabedissen, A., Entchev, E., Renaud, O. and Gonzalez-Gaitan, M. (2006). Sara endosomes and the maintenance of Dpp signaling levels across mitosis. *Science* **314**, 1135-1139.
Brennecke, J., Hipfner, D. R., Stark, A., Russell, R. B. and Cohen, S. M. (2003). bantam encodes a developmentally regulated microRNA that controls cell proliferation and regulates the proapoptotic gene hid in Drosophila. *Cell* **113**, 25-36.
Buszczak, M., Paterno, S., Lighthouse, D., Bachman, J., Planck, J., Owen, S., Skora, A. D., Nystul, T. G., Ohlstein, B., Allen, A. et al. (2007). The carnegie protein trap library: a versatile tool for Drosophila developmental studies. *Genetics* **175**, 1505-1531.
Carrozzino, F., Soulié, P., Huber, D., Mensi, N., Orci, L., Cano, A., Féraille, E. and Montesano, R. (2005). Inducible expression of Snail selectively increases paracellular ion permeability and differentially modulates tight junction proteins. *Am. J. Physiol. Cell Physiol.* **289**, C1002-C1014.
Davis, B. N., Hilyard, A. C., Lagna, G. and Hata, A. (2008). SMAD proteins control DROSHA-mediated microRNA maturation. *Nature* **454**, 56-61.
Deligiannaki, M., Casper, A. L., Jung, C. and Gaul, U. (2015). Pasiflora proteins are novel core components of the septate junction. *Development* **142**, 3046-3057.
Derynck, R., Gelbart, W. M., Harland, R. M., Heldin, C.-H., Kern, S. E., Massagué, J., Melton, D. A., Mlodzik, M., Padgett, R. W., Roberts, A. B. et al. (1996). Nomenclature: vertebrate mediators of TGFbeta family signals. *Cell* **87**, 173.
Doumpas, N., Ruiz-Romero, M., Blanco, E., Edgar, B., Corominas, M. and Teleman, A. A. (2013). Brk regulates wing disc growth in part via repression of Myc expression. *EMBO Rep.* **14**, 261-268.
Enderle, D., Beisel, C., Stadler, M. B., Gerstung, M., Athri, P. and Paro, R. (2011). Polycomb preferentially targets stalled promoters of coding and noncoding transcripts. *Genome Res.* **21**, 216-226.
Faivre-Sarrailh, C., Banerjee, S., Li, J., Hortsch, M., Laval, M. and Bhat, M. A. (2004). Drosophila contactin, a homolog of vertebrate contactin, is required for septate junction organization and paracellular barrier function. *Development* **131**, 4931-4942.
Fehon, R. G., Dawson, I. A. and Artavanis-Tsakonas, S. (1994). A Drosophila homologue of membrane-skeleton protein 4.1 is associated with septate junctions and is encoded by the coracle gene. *Development* **120**, 545-557.
Fristrom, D. K. (1982). Septate junctions in imaginal disks of Drosophila: a model for the redistribution of septa during cell rearrangement. *J. Cell Biol.* **94**, 77-87.
Genova, J. L. and Fehon, R. G. (2003). Neuroglian, Gliotactin, and the Na+/K+ ATPase are essential for septate junction function in Drosophila. *J. Cell Biol.* **161**, 979-989.
Gregory, P. A., Bert, A. G., Paterson, E. L., Barry, S. C., Tsykin, A., Farshid, G., Vadas, M. A., Khew-Goodall, Y. and Goodall, G. J. (2008). The miR-200 family and miR-205 regulate epithelial to mesenchymal transition by targeting ZEB1 and SIP1. *Nat. Cell Biol.* **10**, 593-601.
Haerry, T. E., Khalsa, O., O'Connor, M. B. and Wharton, K. A. (1998). Synergistic signaling by two BMP ligands through the SAX and TKV receptors controls wing growth and patterning in Drosophila. *Development* **125**, 3977-3987.
Hall, S., Bone, C., Oshima, K., Zhang, L., McGraw, M., Lucas, B., Fehon, R. G. and Ward, R. E. (2014). Macroglobulin complement-related encodes a protein required for septate junction organization and paracellular barrier function in Drosophila. *Development* **141**, 889-898.
Harris, R. E. and Ashe, H. L. (2011). Cease and desist: modulating short-range Dpp signalling in the stem-cell niche. *EMBO Rep.* **12**, 519-526.
Herranz, H., Hong, X. and Cohen, S. M. (2012). Mutual repression by bantam miRNA and Capicua links the EGFR/MAPK and Hippo pathways in growth control. *Curr. Biol.* **22**, 651-657.
Inoue, H., Imamura, T., Ishidou, Y., Takase, M., Udagawa, Y., Oka, Y., Tsuneizumi, K., Tabata, T., Miyazono, K. and Kawabata, M. (1998). Interplay of signal mediators of decapentaplegic (Dpp): molecular characterization of mothers against dpp, Medea, and daughters against dpp. *Mol. Biol. Cell* **9**, 2145-2156.
Iovino, N., Pane, A. and Gaul, U. (2009). miR-184 has multiple roles in Drosophila female germline development. *Dev. Cell* **17**, 123-133.
Jovanovic, M. and Hengartner, M. O. (2006). miRNAs and apoptosis: RNAs to die for. *Oncogene* **25**, 6176-6187.
Kapsimali, M., Kloosterman, W. P., de Bruijn, E., Rosa, F., Plasterk, R. H. and Wilson, S. W. (2007). MicroRNAs show a wide diversity of expression profiles in the developing and mature central nervous system. *Genome Biol.* **8**, R173.
Kato, M., Putta, S., Wang, M., Yuan, H., Lanting, L., Nair, I., Gunn, A., Nakagawa, Y., Shimano, H., Todorov, I. et al. (2009). TGF-beta activates Akt kinase through a microRNA-dependent amplifying circuit targeting PTEN. *Nat. Cell Biol.* **11**, 881-889.
Kertesz, M., Iovino, N., Unnerstall, U., Gaul, U. and Segal, E. (2007). The role of site accessibility in microRNA target recognition. *Nat. Genet.* **39**, 1278-1284.
Kheradpour, P., Stark, A., Roy, S. and Kellis, M. (2007). Reliable prediction of regulator targets using 12 Drosophila genomes. *Genome Res.* **17**, 1919-1931.
Leaman, D., Chen, P. Y., Fak, J., Yalcin, A., Pearce, M., Unnerstall, U., Marks, D. S., Sander, C., Tuschl, T. and Gaul, U. (2005). Antisense-mediated depletion reveals essential and specific functions of microRNAs in Drosophila development. *Cell* **121**, 1097-1108.
Li, P., Peng, J., Hu, J., Xu, Z., Xie, W. and Yuan, L. (2011). Localized expression pattern of miR-184 in Drosophila. *Mol. Biol. Rep.* **38**, 355-358.
Livak, K. J. and Schmittgen, T. D. (2001). Analysis of relative gene expression data using real-time quantitative PCR and the 2(-Delta Delta C(T)) Method. *Methods* **25**, 402-408.
Loya, C. M., Lu, C. S., Van Vactor, D. and Fulga, T. A. (2009). Transgenic microRNA inhibition with spatiotemporal specificity in intact organisms. *Nat. Methods* **6**, 897-903.
Martín, F. A., Perez-Garijo, A., Moreno, E. and Morata, G. (2004). The brinker gradient controls wing growth in Drosophila. *Development* **131**, 4921-4930.
Michel, M., Raabe, I., Kupinski, A. P., Pérez-Palencia, R. and Bökel, C. (2011). Local BMP receptor activation at adherens junctions in the Drosophila germline stem cell niche. *Nat. Commun.* **2**, 415.
Newfeld, S. J., Chartoff, E. H., Graff, J. M., Melton, D. A. and Gelbart, W. M. (1996). Mothers against dpp encodes a conserved cytoplasmic protein required in DPP/TGF-beta responsive cells. *Development* **122**, 2099-2108.
Ni, J.-Q., Liu, L.-P., Binari, R., Hardy, R., Shim, H.-S., Cavallaro, A., Booker, M., Pfeiffer, B. D., Markstein, M., Wang, H. et al. (2009). A Drosophila resource of transgenic RNAi lines for neurogenetics. *Genetics* **182**, 1089-1100.
Noirot-Timothée, C., Graf, F. and Noirot, C. (1982). The specialization of septate junctions in regions of tricellular junctions. II. Pleated septate junctions. *J. Ultrastruct. Res.* **78**, 152-165.
Ogiso, Y., Tsuneizumi, K., Masuda, N., Sato, M. and Tabata, T. (2011). Robustness of the Dpp morphogen activity gradient depends on negative feedback regulation by the inhibitory Smad, Dad. *Dev. Growth Differ.* **53**, 668-678.
Oh, H. and Irvine, K. D. (2011). Cooperative regulation of growth by Yorkie and Mad through bantam. *Dev. Cell* **20**, 109-122.
Oshima, K. and Fehon, R. G. (2011). Analysis of protein dynamics within the septate junction reveals a highly stable core protein complex that does not include the basolateral polarity protein Discs large. *J. Cell Sci.* **124**, 2861-2871.
Padash-Barmchi, M., Charish, K., Que, J. and Auld, V. J. (2013). Gliotactin and Discs large are co-regulated to maintain epithelial integrity. *J. Cell Sci.* **126**, 1134-1143.
Padash-Barmchi, M., Browne, K., Sturgeon, K., Jusiak, B. and Auld, V. J. (2010). Control of Gliotactin localization and levels by tyrosine phosphorylation and endocytosis is necessary for survival of polarized epithelia. *J. Cell Sci.* **123**, 4052-4062.
Park, S.-M., Gaur, A. B., Lengyel, E. and Peter, M. E. (2008). The miR-200 family determines the epithelial phenotype of cancer cells by targeting the E-cadherin repressors ZEB1 and ZEB2. *Genes Dev.* **22**, 894-907.
Parker, L., Ellis, J. E., Nguyen, M. Q. and Arora, K. (2006). The divergent TGF-beta ligand Dawdle utilizes an activin pathway to influence axon guidance in Drosophila. *Development* **133**, 4981-4991.
Parnas, D., Haghighi, A. P., Fetter, R. D., Kim, S. W. and Goodman, C. S. (2001). Regulation of postsynaptic structure and protein localization by the Rho-type guanine nucleotide exchange factor dPix. *Neuron* **32**, 415-424.
Paul, S. M., Ternet, M., Salvaterra, P. M. and Beitel, G. J. (2003). The Na+/K+ ATPase is required for septate junction function and epithelial tube-size control in the Drosophila tracheal system. *Development* **130**, 4963-4974.
Petzoldt, A. G., Gleixner, E. M., Fumagalli, A., Vaccari, T. and Simons, M. (2013). Elevated expression of the V-ATPase C subunit triggers JNK-dependent cell invasion and overgrowth in a Drosophila epithelium. *Dis. Models Mech.* **6**, 689-700.
Rorth, P. (1996). A modular misexpression screen in Drosophila detecting tissue-specific phenotypes. *Proc. Natl. Acad. Sci. USA* **93**, 12418-12422.
Ryan, D. G., Oliveira-Fernandes, M. and Lavker, R. M. (2006). MicroRNAs of the mammalian eye display distinct and overlapping tissue specificity. *Mol. Vis.* **12**, 1175-1184.
Saj, A. and Lai, E. C. (2011). Control of microRNA biogenesis and transcription by cell signaling pathways. *Curr. Opin. Genet. Dev.* **21**, 504-510.
Schneider, C. A., Rasband, W. S. and Eliceiri, K. W. (2012). NIH Image to ImageJ: 25 years of image analysis. *Nat. Methods* **9**, 671-675.
Schulte, J., Tepass, U. and Auld, V. J. (2003). Gliotactin, a novel marker of tricellular junctions, is necessary for septate junction development in Drosophila. *J. Cell Biol.* **161**, 991-1000.
Schulte, J., Charish, K., Que, J., Ravn, S., MacKinnon, C. and Auld, V. J. (2006). Gliotactin and Discs large form a protein complex at the tricellular junction of polarized epithelial cells in Drosophila. *J. Cell Sci.* **119**, 4391-4401.
Schwank, G., Restrepo, S. and Basler, K. (2008). Growth regulation by Dpp: an essential role for Brinker and a non-essential role for graded signaling levels. *Development* **135**, 4003-4013.
Stark, A., Brennecke, J., Russell, R. B. and Cohen, S. M. (2003). Identification of Drosophila MicroRNA targets. *PLoS Biol.* **1**, e60.
Sun, Y. H., Tsai, C. J., Green, M. M., Chao, J. L., Yu, C. T., Jaw, T. J., Yeh, J. Y. and Bolshakov, V. N. (1995). White as a reporter gene to detect transcriptional silencers specifying position-specific gene expression during Drosophila melanogaster eye development. *Genetics* **141**, 1075-1086.
Takaesu, N. T., Herbig, E., Zhitomersky, D., O'Connor, M. B. and Newfeld, S. J. (2005). DNA-binding domain mutations in SMAD genes yield dominant-negative proteins or a neomorphic protein that can activate WG target genes in Drosophila. *Development* **132**, 4883-4894.

Journal of Cell Science

Teleman, A. A. and Cohen, S. M. (2000). Dpp gradient formation in the Drosophila wing imaginal disc. *Cell* **103**, 971-980.
Tepass, U. and Hartenstein, V. (1994). The development of cellular junctions in the Drosophila embryo. *Dev. Biol.* **161**, 563-596.
Tsukita, S., Furuse, M. and Itoh, M. (2001). Multifunctional strands in tight junctions. *Nat. Rev. Mol. Cell Biol.* **2**, 285-293.
Venema, D. R., Zeev-Ben-Mordehai, T. and Auld, V. J. (2004). Transient apical polarization of Gliotactin and Coracle is required for parallel alignment of wing hairs in Drosophila. *Dev. Biol.* **275**, 301-314.
Wang, F. E., Zhang, C., Maminishkis, A., Dong, L., Zhi, C., Li, R., Zhao, J., Majerciak, V., Gaur, A. B., Chen, S. et al. (2010). MicroRNA-204/211 alters epithelial physiology. *FASEB J.* **24**, 1552-1571.
Winbanks, C. E., Wang, B., Beyer, C., Koh, P., White, L., Kantharidis, P. and Gregorevic, P. (2011). TGF-beta regulates miR-206 and miR-29 to control myogenic differentiation through regulation of HDAC4. *J. Biol. Chem.* **286**, 13805-13814.
Xu, P., Vernooy, S. Y., Guo, M. and Hay, B. A. (2003). The Drosophila microRNA Mir-14 suppresses cell death and is required for normal fat metabolism. *Curr. Biol.* **13**, 790-795.
Xu, J., Lamouille, S. and Derynck, R. (2009). TGF-beta-induced epithelial to mesenchymal transition. *Cell Res.* **19**, 156-172.
Yang, M., Lee, J.-E., Padgett, R. W. and Edery, I. (2008). Circadian regulation of a limited set of conserved microRNAs in Drosophila. *BMC Genomics* **9**, 83.
Ye, D., Guo, S., Al-Sadi, R. and Ma, T. Y. (2011). MicroRNA regulation of intestinal epithelial tight junction permeability. *Gastroenterology* **141**, 1323-1333.
Yu, J., Ryan, D. G., Getsios, S., Oliveira-Fernandes, M., Fatima, A. and Lavker, R. M. (2008). MicroRNA-184 antagonizes microRNA-205 to maintain SHIP2 levels in epithelia. *Proc. Natl. Acad. Sci. USA* **105**, 19300-19305.
Zhang, X., Luo, D., Pflugfelder, G. O. and Shen, J. (2013). Dpp signaling inhibits proliferation in the Drosophila wing by Omb-dependent regional control of bantam. *Development* **140**, 2917-2922.